MULTI-OBJECTIVE CALIBRATION OF THE DOUBLE-ELLIPSOID HEAT SOURCE MODEL FOR GMAW PROCESS SIMULATION

by

Mišo B. BJELIĆ[a], Branko S. RADIČEVIĆ[a*], Karel KOVANDA[b], Ladislav KOLARIK[b], and Aleksandra V. PETROVIĆ[a]

[a] Faculty of Mechanical and Civil Engineering in Kraljevo, University of Kragujevac, Kraljevo, Serbia
[b] Faculty of Mechanical Engineering, Czech Technical University in Prague, Prague, Czech Republic

Original scientific paper
https://doi.org/10.2298/TSCI210131181B

The scope of application of simulation models in welding is limited by the accuracy of their output results. This paper presents a calibration procedure for a 3-D quasi-stationary model of heat transfer for gas metal arc welding. The double-ellipsoid heat source used in this model has five input parameters whose value cannot be specified accurately. To estimate these values, we employed a multi-objective calibration procedure with two objective functions using the paretosearch optimization algorithm. Objective functions represented the error between simulated and experimentally observed values of penetration depth and weld bead width during gas metal arc welding of P355GH steel plates. All input parameters were assumed to be a power function of line energy. To reduce computational time, we replaced the numerical model with a response surface methodology metamodel based on an optimal set of simulation results from the numerical model. The results of the simulations based on calculated values of input parameters for the heat source model showed excellent matching with the experimental results.

Key words*: welding simulation, multi-objective calibration, double-ellipsoid heat source, RSM*

Introduction

Although simulation modelling of different production processes has a growing trend in recent years, the application of simulation models of welding processes is still limited. The main reason is a lack of knowledge of correct values of some input parameters, which in turn provides insufficiently reliable output results regardless of the complexity of the model. In the case of the welding heat transfer model, the parameters that most affect the accuracy of the output results are the parameters related to the model of a heat source. Widely used Goldak's double-ellipsoid heat source [1], is defined by five input parameters neglecting the power of the heat source, fig. 1. The first of those five parameters is arc efficiency. For the GMAW process, the value of arc efficiency varies from 0.80 to 0.88 in the case of Ar shielding [2]. In the case of 90% Ar to 10% CO_2 shielding, arc efficiency was found to be in the range from 0.68-0.86 [3]. Some authors have reported values between 0.675 and 0.722 [4]. It is obvious that such wide limits for arc efficiency significantly affect the results of the simulation.

* Corresponding author, e-mail: radicevic.b@mfkv.kg.ac.rs

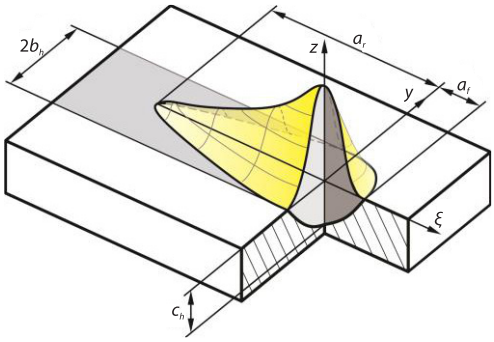

Figure 1. Double-ellipsoid heat source

The other four parameters a_f, a_r, b_h and c_h are the semiaxes of the front and rear ellipsoid, fig 1. Power of the heat source is distributed, eqs. (1)-(3), between the front and rear ellipsoid in a ratio which corresponds to values of parameters $f_f = 2a_f/(a_f + a_r)$ and $f_r = 2a_r/(a_f + a_r)$ [5]:

$$q_f(x,y,z) = \frac{6\sqrt{3} f_f Q}{a_f b_h c_h \pi\sqrt{\pi}} e^{-3\frac{x^2}{a_f^2}} e^{-3\frac{y^2}{b_h^2}} e^{-3\frac{z^2}{c_h^2}} \tag{1}$$

$$q_r(x,y,z) = \frac{6\sqrt{3} f_r Q}{a_r b_h c_h \pi\sqrt{\pi}} e^{-3\frac{x^2}{a_r^2}} e^{-3\frac{y^2}{b_h^2}} e^{-3\frac{z^2}{c_h^2}} \tag{2}$$

$$Q = \eta UI \tag{3}$$

Goldak *et al.* [1] suggested that the value of parameters b_h and c_h should be measured directly from an experimental cross-section of the weld. They also suggested that in absence of experimental data Christensen's [6] expressions could be used. For f_f and f_r they proposed values of 0.6 and 1.4, respectively. Joshi *et al.* [7] assumed that $f_f = 0.48$ and $f_r = 1.52$ while Chen *et al.* [8] as well as Jia *et al.* [9] suggested that values of parameters f_f and f_r should be 0.5 and 1.5, respectively. Guided by Goldak's [10] recommendation, Nasiri and Enzinger [11] have used parameters of double-ellipsoid heat source about 10% smaller than actual weld geometry.

For reliable output results of the simulation model, it is necessary to determine the exact values of these input parameters. In the case of individual simulations, we can achieve this goal, minimizing the error between the simulation and experimental results by combining the simulation model with some multivariable optimization algorithm [12-18]. The complexity of the problem arises when it is necessary to determine the optimal values of these parameters for several different simulations [19]. In this case, it is possible to assume that there is a functional dependence between the heat source parameters and some of the process parameters [9, 19, 20]. This way, we can determine the values of input parameters for the whole interval of different simulation conditions. The use of multi-objective [21, 22] instead of single-objective optimization algorithm [14, 23-25] allows the error estimation for each parameter included in the objective functions separately. That gives us the possibility to choose the appropriate functional relations depending on the need for the greater or lesser error of individual parameters concerning experimental results.

The application of numerical models in simulations of the welding process is practically impossible without the use of computers. Despite the development of computer technology, welding simulations still require a large amount of time to perform. However, in a situation such as model calibration or some form of optimization, the number of simulation runs can be large, which in turn leads to a very long time required to obtain the final results. Therefore, it makes sense to use metamodels as an efficient replacement for numerical models. The most commonly used metamodelling techniques are regression analysis [23, 26-28] and neural networks [29-31].

In this article, we proposed an RSM metamodel based calibration methodology for the reduction of the error between simulated and experimental weld penetration depth and weld bead width. This calibration methodology implied the determination of heat source parameters as functions of line energy. The RSM metamodel was used as a replacement for the numerical heat transfer model to reduce the computational time.

This way, we were able to use a multi-objective paretosearch optimization algorithm to calculate the values of double-ellipsoid heat source parameters for multiple simulation conditions.

Heat transfer analysis

The heat transfer during welding, can be described with a non-stationary, partial differential equation, eq. (4) [22], where ρ, c_p, and λ are density, specific heat capacity and thermal conductivity of material while L and q_l are latent heat of melting/solidification and volumetric heat source described by Goldak's double-ellipsoid model. An analytical solution for this type of equation is connected with difficulties related to non-linearities of material physical properties, the complexity of boundary conditions, and the heat source model:

$$\rho c_p \frac{\partial T}{\partial t} = \lambda\left(\frac{\partial^2 T}{\partial x^2}+\frac{\partial^2 T}{\partial y^2}+\frac{\partial^2 T}{\partial z^2}\right)-\rho L\frac{\partial f_{\text{liq}}}{\partial t}+q_l \tag{4}$$

Latent heat of melting/solidification is described using liquid phase fraction in mushy zone between solidus T_{sol}, and liquidus temperature T_{liq}, eq. (5):

$$f_{\text{liq}} = \begin{cases} 0 & \text{for} \quad T \le T_{\text{sol}} \\ \dfrac{T-T_{\text{sol}}}{T_{\text{liq}}-T_{\text{sol}}} & \text{for} \quad T_{\text{sol}} < T < T_{\text{liq}} \\ 1 & \text{for} \quad T \ge T_{\text{liq}} \end{cases} \tag{5}$$

In case of constant welding speed, v_{w}, it is possible to transform eq. (4) to the quasi-steady-state form, eq. (7). This kind of transformation requires the application of a moving co-ordinate system ξyz, fig. 2. The connection between co-ordinate systems xyz and ξyz is defined:

$$\xi = x - v_w t \tag{6}$$

Considering eqs. (4) and (6), heat transfer eq. (7) in moving co-ordinate system can be written:

$$-v_{\text{w}} c_{\text{eff}} \frac{\partial T}{\partial \xi} = \frac{\lambda}{\rho c_p}\left(\frac{\partial^2 T}{\partial \xi^2}+\frac{\partial^2 T}{\partial y^2}+\frac{\partial^2 T}{\partial z^2}\right)+q_l \tag{7}$$

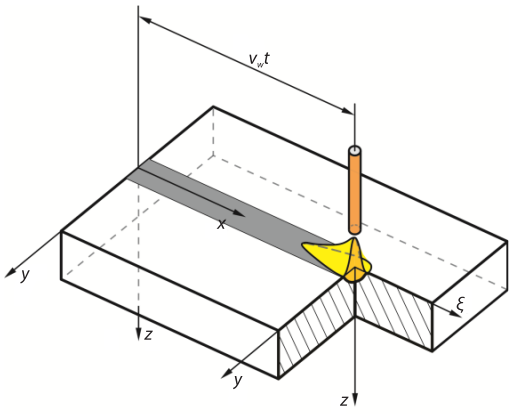

Figure 2. Moving co-ordinate system

where c_{eff} is effective heat capacity:

$$c_{eff} = \left(1+\frac{L}{c_p}\frac{\partial f_{liq}}{\partial T}\right) \tag{8}$$

Equation (7) is solved in MATLAB iteratively, using the multigrid and the successive over-relaxation finite differences method.

Experimental procedure

The calibration procedure was performed using experimental data from specimens with dimensions 300 mm × 150 mm × 5.3 mm. The base material for specimens was P355GH steel with the chemical composition given in tab. 1. The filler material used was OK Autrod

12.50 uncoated wire with a diameter of 1.2 mm. As a shielding gas, a two-component mixture of 82% Ar and 18% CO_2 was used. Four specimens were welded in a flat position using ARC Mate 100iC welding robot with Migatronic Sigma Galaxy 400 power source.

Table 1. Chemical composition of base material - P355GH

C	Si	P	S	Mn	Nb
0.20	0.19	0.016	0.062	1.45	0.014

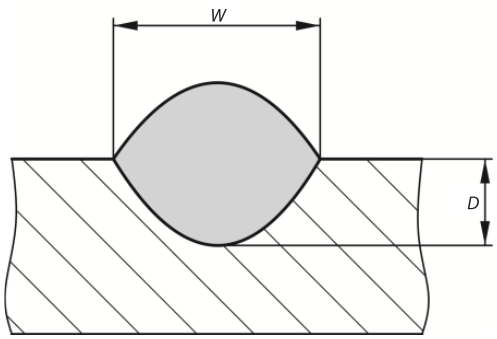

Figure 3. Measured weld geometry

For each of four specimens, single pass bead on plate weld was made along the centerline. Welding parameters for all specimens are listed in tab. 2. After welding, macrograph sections were prepared to measure weld geometry dimensions. Two dimensions were measured: weld bead width and depth of penetration, fig. 3. Measurements were made using a STEMI DV-4 stereo microscope with an integrated AxioCam Erc 5s camera. For calibration purposes, only data from specimens I and IV were used, while specimens II and III were intended for model validation, tab. 3.

Table 2. Welding parameters

Parameter	Specimen			
	I	II	III	IV
Voltage [V]	20.2	20.3	21.2	21.8
Current [A]	185	190	208	222
Welding speed [mms^{-1}]	8	8	8	8
Wire feed rate [m per minute]	4.3	4.5	5.2	5.7
Wire diameter [mm]	1.2	1.2	1.2	1.2
Gas-flow [Lpm]	12	12	12	12

Table 3. Measured weld dimensions

Parameter	Specimen			
	I	II	III	IV
W [mm]	6.5	6.6	7.2	7.3
D [mm]	2.1	2.1	2.4	2.3

Metamodelling

Metamodelling represents a technique by which a particular model is replaced by another that appropriately imitates the original model, and at the same time, has better characteristics related to computational efficiency [32].

Solving eq. (7) iteratively using the finite differences method is associated with a large number of iterations, which results in a large computational time. Bearing in mind that the calibration process is based on the multi-objective optimization method, this further increases the

time required to reach a solution. In this case, an RSM-based metamodel is employed to reduce the computational time.

Based on the welding parameters shown in tab. 2, for specimens I and IV, and using the Design-Expert software package, an I-optimal plan of experiments was created. As already mentioned, Goldak's model has five unknown input parameters: η, a_f, a_r, b_h, and c_h. To reduce the number of experimental runs it is assumed that parameters a_f and b_h are equal. Therefore, the following variables were used as input ones:

$$x_1 = \eta,\ x_2 = b_h/b_{hexp},\ x_3 = c_h/c_{hexp},\ x_4 = a_r/a_f$$

Levels of input parameters are listed in tab. 4.

Table 4. Levels of input parameters

Levels	Factors			
	x_1	x_2	x_3	x_4
Level 1	0.6	0.9	0.9	2
Level 2	0.9	1.1	1.1	4

We have used numerical model based on eq. (7) to calculate values of weld bead width and penetration depth for specimens I and IV using design matrix, tab. 5, and values of welding parameters listed in tab. 2.

Table 5. Optimal design matrix

Run	Factors				Responses [mm]			
	x_1	x_2	x_3	x_4	W_I	D_I	W_{IV}	D_{IV}
1	0.9	0.954	1.1	2.52	6.2	2.7	6.9	3.1
2	0.6	0.9	0.9	4	4.5	1.7	5.4	2.2
3	0.6	1.1	0.9	2	5.6	1.9	6.5	2.2
4	0.6	0.9	1.1	2	5.1	2.3	5.9	2.5
5	0.723	0.9	0.955	2	5.8	2.3	6.4	2.7
6	0.759	1.01891	0.9	3.2	5.9	2.2	6.6	2.4
7	0.615	1.1	1.1	2.6	4.8	1.7	6.1	2.4
8	0.9	1.1	0.951	2.54	6.6	2.4	7.3	2.6
9	0.616395	1.1	0.959	4	4.7	1.6	5.5	1.9
10	0.9	0.9	0.9	2	6.3	2.5	7.3	3.1
11	0.6	1.1	1.1	4	4	1.5	5.3	2
12	0.615	0.96	1.1	4	4.4	1.8	5.4	2.2
13	0.834	1.023	1.023	3.24329	5.9	2.4	6.8	2.8
14	0.68871	0.982	1.1	2.8	5.3	2.2	6.2	2.6
15	0.9	0.952	0.952901	4	5.9	2.5	6.6	2.7
16	0.84	1.1	1.1	4	5.6	2.2	6.5	2.7
17	0.760449	1.021	1.02	2	5.9	2.3	6.9	2.8
18	0.6	0.971	0.972	2.7	5.1	1.9	5.8	2.3
19	0.9	1.1	0.921	4	6.2	2.3	6.9	2.6
20	0.7605	0.9	1.022	3.2	5.5	2.4	6.2	2.6

Mathematical metamodels of functional relations between weld geometry and parameters x_1 to x_4 for specimens I and IV were obtained using the Design-Expert software package. For specimen I, weld bead width W_I and penetration depth D_I are described by 2FI models. Models are power transformed:

$$W_I = \left(-506.919 - 294.903x_1 + 780.403x_2 + 735.052x_3 - 29.1603x_4 + 583.514x_1x_2 + \right.$$
$$\left. + 133.67x_1x_3 - 4.88747x_1x_4 - 1058.41x_2x_3 - 22.4403x_2x_4 + 26.0028x_3x_4\right)^{1/3} \quad (9)$$

$$D_I = \left(-45.3105 + 1.86122x_1 + 50.8888x_2 + 50.098x_3 - 1.25343x_4 - 9.2795x_1x_2 + \right.$$
$$\left. + 16.3006x_1x_3 + 1.83625x_1x_4 - 54.3195x_2x_3 + 0.486464x_2x_4 - 1.16573x_3x_4\right)^{1/2.32} \quad (10)$$

Comparation of experimental and predicted values of parameters W_I and D_I are shown in figs. 4. and 5, respectively. Based on these figures, it is clear that both metamodels represent a good replacement for the numerical model.

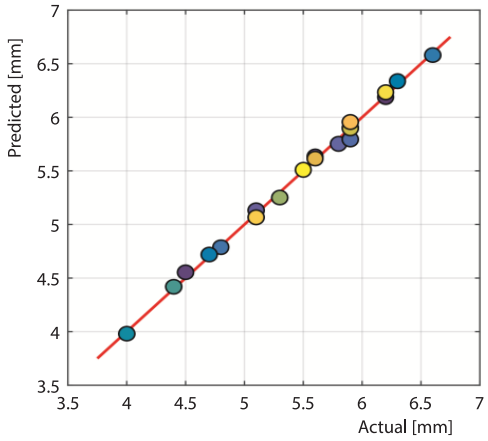

Figure 4. Predicted *vs.* actual scatter plot for parameter W_I

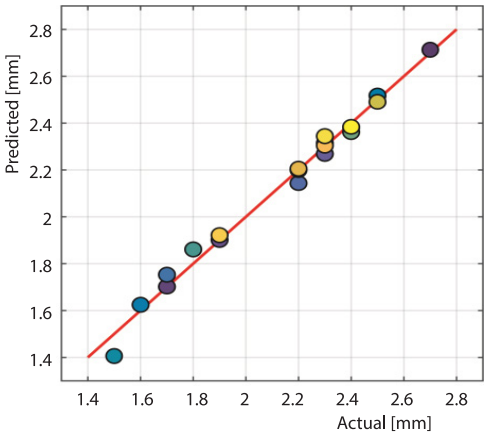

Figure 5. Predicted *vs.* actual scatter plot for parameter D_I

Similarly, for specimen IV, weld bead width W_{IV} and penetration depth D_{IV} can be described by power transformed linear models:

$$W_{IV} = \left(9.14992 + 96.5959x_1 + 36.8124x_2 - 24.4857x_3 - 8.51831x_4\right)^{1/2.27} \quad (11)$$

$$D_{IV} = \left(1.52052 + 2.58036x_1 - 1.27186x_2 + 1.12647x_3 - 0.174858x_4\right)^{1/1.09} \quad (12)$$

Comparison between actual and predicted values for parameters W_{IV} and D_{IV} is shown in figs. 6. and 7, respectively. The adequacy for all models is tested using the statistical analysis of variance (ANOVA). Results of ANOVA are shown in tab. 6. The *F*-values of models imply that all models are significant while low *P*-values less than 0.05 indicate model terms are significant. The predicted R^2 is in reasonable agreement with the adjusted R^2 for all models.

Table 6. The ANOVA analysis for metamodels W_I, D_I, W_{IV}, and D_{IV}

Model	SS	df	MS	*F*	*p*	R^2	Adj. R^2	Pred. R^2	Adeq *P*
W_I	70766.92	10	7076.69	229.39	< 0.0001	0.9961	0.9917	0.9687	53.8446
D_I	81.49	10	8.15	97.45	< 0.0001	0.9908	0.9807	0.9335	36.9678
W_{IV}	3924.10	4	981.03	171.90	< 0.0001	0.9787	0.9730	0.9628	40.8285
D_{IV}	2.62	4	0.6551	57.91	< 0.0001	0.9392	0.9230	0.8835	25.1054

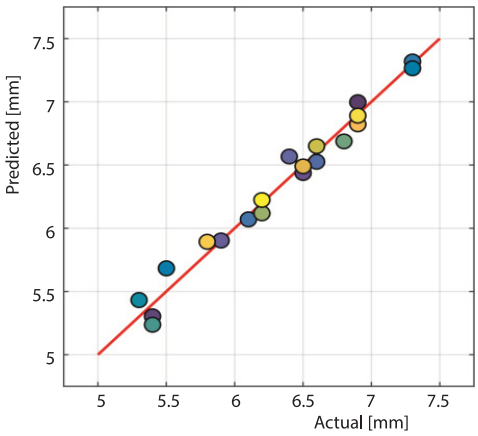

Figure 6. Predicted *vs.* actual scatter plot for parameter W_{IV}

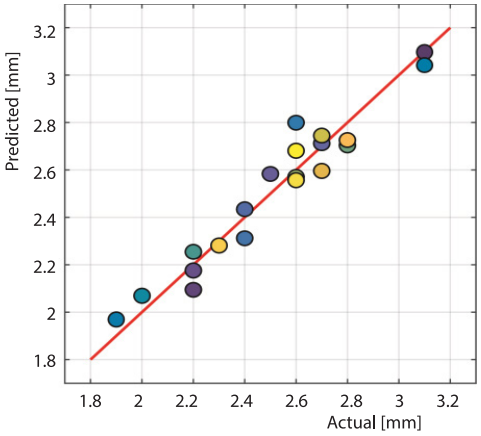

Figure 7. Predicted *vs.* actual scatter plot for parameter D_{IV}

Optimization methodology

Multi-objective optimization methods involve simultaneous optimization of two or more objective functions instead of optimization of the single objective as a linear combination of multiple objective functions. This way, it is possible to estimate each objective function separately, which gives us the possibility to choose the appropriate solution. In this case, that means that we can choose the solution with smaller or larger error either for one or multiple objective functions.

The optimization procedure was performed using the MATLAB software package and paretosearch algorithm. This algorithm uses pattern search on a set of points to search iteratively for non-dominated solutions [33].

Objective O_1 and O_2 are defined using least-squares method, tab. 7. Here, $W_j^{\exp}$ and $D_j^{\exp}$ are measured values of weld bead width and penetration depth for specimens I and IV, tab. 3, and j is number of specimens used for calibration, in this case, $j = 2$.

Table 7. Objective functions

$O_1(x_1, x_2, x_3, x_4)$	$O_2(x_1, x_2, x_3, x_4)$
$\sum_{j=1}^{2}\left(\frac{W_j^{\exp} - W_j^{\sin}}{W_j^{\exp}}\right)^2$	$\sum_{j=1}^{2}\left(\frac{D_j^{\exp} - D_j^{\sin}}{D_j^{\exp}}\right)^2$

As the unknown parameters, variables x_1, x_2, x_3, and x_4 have been chosen. We intended to determine if there is a functional relations between variables x_1, x_2, x_3, x_4, and welding parameters. So we assumed the following relations between them, tab. 8.

Table 8. Assumed functional relations

Variables			
$x_1 = a_1 + b_1\left(\frac{UI}{v_w}\right)^{c_1}$	$x_2 = a_2 + b_2\left(\frac{U_I}{v_w}\right)^{c_2}$	$x_3 = a_3 + b_3\left(\frac{U_I}{v_w}\right)^{c_3}$	$x_4 = a_4 + b_4\left(\frac{U_I}{v_w}\right)^{c_4}$

All functional relations were supposed to be a power function of line energy, where U is arc voltage, I – the arc current, v_w – the welding speed, and a_i, b_i, and c_i are unknown con-

stants. The main goal of the optimization was to determine values of constants a_i, b_i, and c_i so that differences between experimental and computed values defined by objective functions, be minimal. The constraints were supposed as follows, tab. 9.

Table 9. Variables constraints

Variables			
$0.6 \le x_1 \le 0.9$	$0.9 \le x_2 \le 1.1$	$0.9 \le x_3 \le 1.1$	$2 \le x_4 \le 4$

The optimization problem can be stated:

$$\min\left[O_1\left(x_1,x_2,x_3,x_4\right),\ O_2\left(x_1,x_2,x_3,x_4\right)\right]$$
$$x_i = a_i + b_i\left(\frac{U_1}{v_w}\right)^{c_i} \tag{13}$$
$$x_{i\min} \le x_i \le x_{i\max}$$

The result of multi-objective optimization is shown in the form of the Pareto front, fig. 8. It contains a set of 1000 non-dominated solutions. It is not possible to directly choose one solution from this set, which is superior to other solutions considering both objective functions. To overcome this problem we have used the Taguchi signal-to-noise ratio ratio. The signal-to-noise ratio implies three categories of performance characteristics: the lower-the-better, the higher-the-better, and the nominal-the-better. The lower-the-better characteristic is used in the case when it is necessary to minimize the response. It can be expressed:

$$\frac{S}{N} = -10\log\left(\frac{1}{n}\sum_{i=1}^{n} Y_i^2\right) \tag{14}$$

where n is the number of observed values, in this case, the number of objective functions, and Y_i is the value of the observed characteristic, *i.e.*, the value of the objective function. For all three performance characteristics, a higher S/N ratio matches to better performance characteristics. In our case, this means that the non-dominated solution with the highest S/N ratio is superior to other solutions. The S/N ratio for a set of non-dominated solutions from Pareto front is shown at fig. 9.

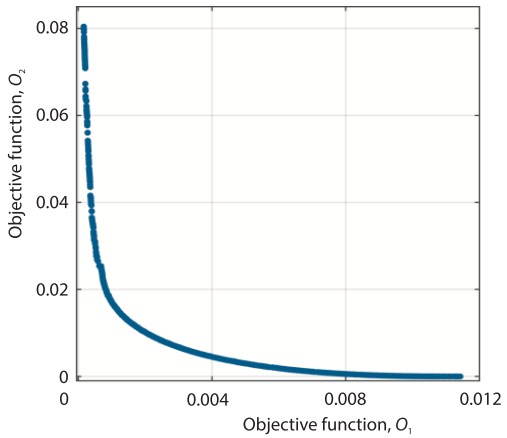

Figure 8. Pareto front of the optimization problem

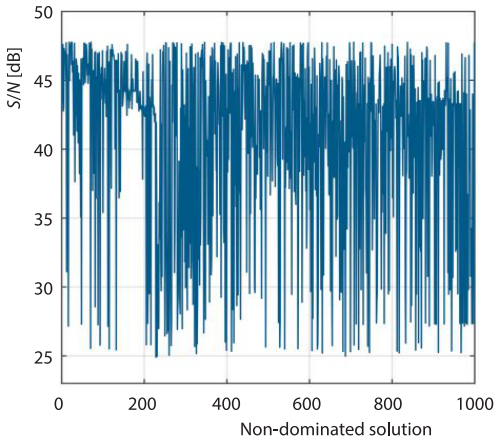

Figure 9. The S/N ratio for all non-dominated solutions

The solution with the highest *S*/*N* ratio of 47.7764 [dB] was chosen as optimal one, from the set of 1000 non-dominated solutions, fig. 9. Values of constants a_i, b_i, and c_i which correspond to the optimal solution are listed in tab. 9.

Table 9. Values of constants a_i, b_i, and c_i

Constants	$i = 1$	$i = 2$	$i = 3$	$i = 4$
a_i	0.0790	1.0999	0.9001	0.5908
b_i	4.4783	$6.0708 \cdot 10^{-6}$	$-3.1099 \cdot 10^{-7}$	1.4094
c_i	–0.3069	0.3564	0.7648	$5.7131 \cdot 10^{-6}$

Functional relations, tab. 8, between parameters

$$x_1 = \eta,\ x_2 = b_h/b_{hexp},\ x_3 = c_h/c_{hexp},\ x_4 = a_r/a_f$$

and line energy are shown on figs. 10 and 11. As can be seen, parameters x_2, x_3, and x_4 have nearly constant values over the whole interval of line energy. The value of parameter x_3, which is 10% smaller than actual weld geometry, is in good agreement with the proposition of Nasiri and Enzinger [11], while the parameter x_2 has a value which is 10% higher than actual geometry. The parameter x_4 has a value of 2, which corresponds to $f_f = 0.67$ and $f_r = 1.33$, and agrees with Nguyen [34]. Only parameter x_1 changes decreasing from the value of 0.76 for specimen I to 0.71 for specimen IV. This corresponds to values of arc efficiency found by Haelsig *et al*. [3].

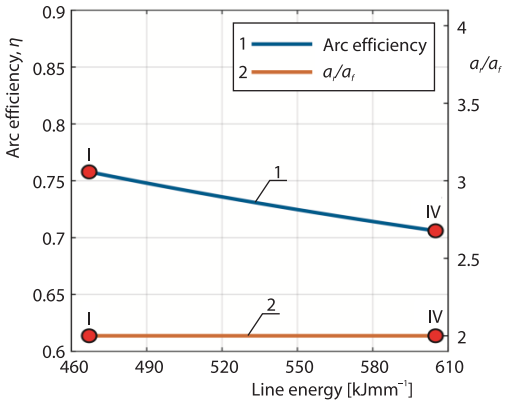

Figure 10. Functional relations for variables x_1 and x_4

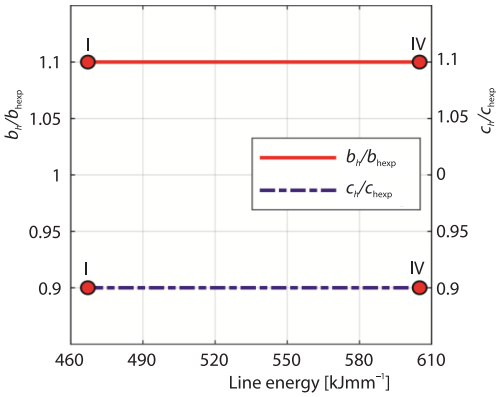

Figure 11. Functional relations for variables x_2 and x_3

Using functional relations, tab. 8, and values of line energy, tab. 2, we have used calculated values of parameters η, b_h, c_h, and a_r/a_f to simulate weld geometry for all specimens. Relative errors for specimens I and IV were 3.1% and 4.1%, respectively. For depth of penetration, relative errors for these two samples were 4.8% and 4.4%. The maximal relative error for the specimens II and III which were used for model validation were 8.3% in case of weld bead for specimen III.

Figures 12 and 13 show simulated weld geometry compared to the experimental one in the case of specimens I and IV. According to tab. 10 and figs. 12 and 13, a calibrated numerical model can reliably predict actual weld geometry.

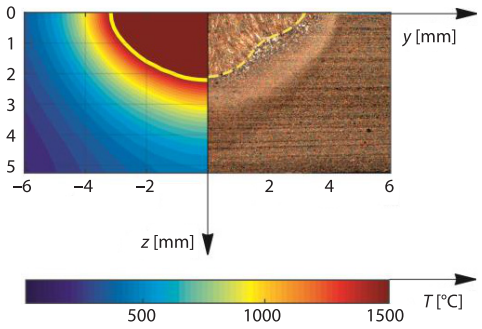

Figure 12. Comparison between simulated and experimental weld bead geometry for specimen I

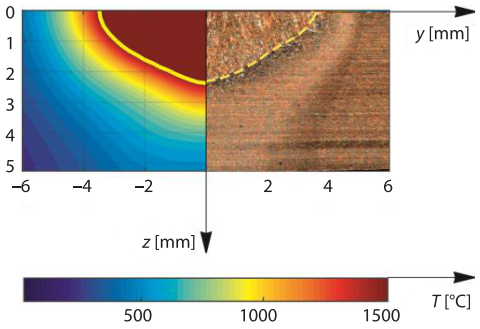

Figure 13. Comparison between simulated and experimental weld bead geometry for specimen IV

Table 10. Absolute and relative errors

Spec.	Parameter							
	Weld bead width [mm]				Depth of penetration [mm]			
	W_{sim}	W_{exp}	Abs. error	Rel. error	D_{sim}	D_{exp}	Abs. error	Rel. error
I	6.3	6.5	0.2	0.031	2.2	2.1	0.1	0.048
II	6.4	6.6	0.2	0.03	2.2	2.1	0.1	0.048
III	6.6	7.2	0.6	0.083	2.4	2.4	0	0
IV	7.0	7.3	0.3	0.041	2.4	2.3	0.1	0.044

Summary and conclusions

To improve the reliability of the 3-D numerical heat transfer model, we have developed a calibration procedure to determine the input parameters of the double-ellipsoid heat source. The procedure were based on a multi-objective paretosearch optimization algorithm combined with RSM metamodel. This approach proved to be an efficient and reliable way to speed up the optimization process. All input parameters were supposed to be power functions of line energy. The results of simulations based on the heat source parameters calculated using the calibration model show good agreement between simulated and actual weld geometry. It leads to the conclusion that the calibration model based on the functional relations between heat source parameters and welding parameters provides a reliable way to increase the accuracy of the output results of the numerical model.

Acknowledgment

The authors wish to express their gratitude to the Ministry of Education, Science and Technological development of the Republic of Serbia for support through contract No. 451-03-68/2020-14/200108 and to the National CEEPUS Office of the Czech Republic through project CIII-HR-0108-07-1314.

Nomenclature

a_f – semiaxis of front half-ellipsoid in x-direction, [m]
a_r – semiaxis of rear half-ellipsoid in x-direction, [m]
b_h – semiaxis of front half-ellipsoid in y-direction, [m]
c_h – semiaxis of front half-ellipsoid in z-direction, [m]
c_{eff} – effective heat capacity
c_p – specific heat capacity, [Jkg^{-1}K^{-1}]
D – depth of penetration [mm]
f_f – front proportion coefficient

f_{liq} – liquid phase fraction, [%]
f_r – rear proportion coefficient
I – welding current, [A]
L – latent heat, [Jkg^{-1}]
n – number of observed values
q_l – heat density, [Wm^{-3}]
O_1 – first objective function
O_2 – second objective function
S/N – signal to noise ratio [dB]
T – temperature, [°C]
Q – arc power, [W]
t – time, [s]
U – arc voltage, [V]
v_w – welding speed, [ms^{-1}]
W – weld bead width [mm]
x – unknown parameters
Y – value of the observed characteristic

Greek symbols

η – arc efficiency, [%]
λ – thermal conductivity, [Wm^{-1}K^{-1}]
ρ – density, [kgm^{-3}]
ξ – axis of moving co-ordinate system

Subscripts

i – i^{th} parameter
I-IV – specimen number
j – number of specimens used for calibration
liq – liquidus
sol – solidus

Superscripts

exp – experimental
sim – simulated

References

[1] Goldak, J., *et al*., A New Finite Element Model For Welding Heat Sources, *Metallurgical Transactions B*, *15* (1984), 2, pp. 299-305
[2] DuPont, J. N., Marder, A. R., Thermal Efficiency Of Arc Welding Processes, *Welding Journal*, *74* (1995), 12, pp. 406-416
[3] Haelsig, A., *et al*., New Findings on the Efficiency of Gas Shielded Arc Welding, *Welding in the World*, *56* (2012), 11-12, pp. 98-104
[4] Joseph, A., *et al*., Measurement and Calculation of Arc Power and Heat Transfer Efficiency in Pulsed Gas Metal Arc Welding, *Science and Technology of Welding and Joining*, *8* (2003), 6, pp. 400-406
[5] Wu, C. S., *Welding Thermal Processes and Weld Pool Behaviors*, Taylor & Francis, Boca Raton, Fla., USA, 2011
[6] Christensen, N., *et al*., Distribution of Temperatures in Arc Welding, *British Welding Journal*, *12* (1965), 2, pp. 54-75
[7] Joshi, S., *et al*., Characterization of Material Properties and Heat Source Parameters in Welding Simulation of Two Overlapping Beads on a Substrate Plate, *Computational Materials Science*, *69* (2013), Mar., pp. 559-565
[8] Chen, B. Q., *et al*., Numerical and Experimental Studies on Temperature and Distortion Patterns in Butt-Welded Plates, *International Journal of Advanced Manufacturing Technology*, *72* (2014), 5-8, pp. 1121-1131
[9] Jia, X., *et al*., A New Method to Estimate Heat Source Parameters in Gas Metal Arc Welding Simulation Process, *Fusion Engineering and Design*, *89* (2014), 1, pp. 40-48
[10] Goldak, J. A., Akhlaghi, M., *Computational Welding Mechanics*, Springer, New York, USA, 2005
[11] Nasiri, M. B., Enzinger, N., Powerful Analytical Solution Heat Flow Problem in Welding, *International Journal of Thermal Sciences*, *135* (2019), Jan., pp. 601-612
[12] Kumar, A., Debroy, T., Tailoring Complex Weld Geometry through Reliable Heat Transfer and Fluid-Flow Calculations and a Genetic Algorithm, Metallurgical and Materials Transactions A: P*hysical Metallurgy and Materials Science*, *36* (2005), 10, pp. 2725-2735
[13] De, A., A Smart Model to Estimate Effective Thermal Conductivity and Viscosity in the Weld Pool, *Journal of Applied Physics*, *95* (2004), 9, pp. 5230-5240
[14] Bag, S., *et al*., Use of a Multivariate Optimization Algorithm to Develop a Self-Consistent Numerical Heat Transfer Model for Laser Spot Welding, *The International Journal of Advanced Manufacturing Technology*, *38* (2007), 5-6, pp. 575-585
[15] Kumar, A., DebRoy, T., Guaranteed Fillet Weld Geometry from Heat Transfer Model and Multivariable Optimization, *International Journal of Heat and Mass Transfer*, *47* (2004), 26, pp. 5793-5806
[16] Gu, Y., *et al*., Determination of Parameters of Double-Ellipsoidal Heat Source Model Based on Optimization Method, *Welding in the World*, *63* (2019), 2, pp. 365-376
[17] Mijajlovic, M., *et al*., Effective Temperature Based Algorithm for Achieving Constant Quality Resistance Seam Weld, *Thermal Science*, *25* (2021), 4A, pp. 2459-2469

[18] Farias, R. M., *et al*., An Efficient Computational Approach for Heat Source Optimization in Numerical Simulations of Arc Welding Processes, *Journal of Constructional Steel Research*, *176* (2021), 106382, pp. 1-13
[19] Lazić, V. N., *et al*., Numerical Analysis of Temperature Field during Hardfacing Process and Comparison with Experimental Results, *Thermal Science*, *18* (2014), Suppl. 1, pp. S113-S120
[20] Kumar, A., DebRoy, T., Improving Reliability of Modelling Heat and Fluid-flow in Complex Gas Metal Arc Fillet Welds – Part II: Application Welding of Steel, *Journal of Physics D: Applied Physics*, *38* (2005), 1, pp. 127-134
[21] Chen, C., *et al*., Study of Heat Source Calibration and Modelling for Laser Welding Process, *International Journal of Precision Engineering and Manufacturing*, *19* (2018), 8, pp. 1239-1244
[22] Bjelić, M., Characterization of Weld Geometry and Microstructure Based on Heat Transfer and Metallurgical Model of the GMAW Process as a Basis for Prediction of the Technological Parameters (in Serbian), Ph. D. thesis, University of Kragujevac, Kraljevo, Serbia, 2016
[23] Correia, D. S., *et al*., Comparison between Genetic Algorithms and Response Surface Methodology in GMAW Welding Optimization, *Journal of Materials Processing Technology*, *160* (2005), 1, pp. 70-76
[24] Islam, M., *et al*., Simulation-Based Numerical Optimization of Arc Welding Process for Reduced Distortion in Welded Structures, *Finite Elements in Analysis and Design*, *84* (2014), July, pp. 54-64
[25] Bjelić, M. B., *et al*., Numerical Modelling of 2-D Heat Transfer and Temperature-Based Calibration Using Simulated Annealing Optimization Method: *Application Gas Metal Arc Welding, Thermal Science*, *20* (2016), 2, pp. 655-665
[26] Martinez-Conesa, E., *et al*., Optimization of Geometric Parameters in a Welded Joint through Response Surface Methodology, *Construction & Building Materials*, *154* (2017), Nov., pp. 105-114
[27] Meseguer-Valdenebro, J., *et al*., Calculation of T8/5 by Response Surface Methodology for Electric Arc Welding Applications, *Thermal Science*, *18* (2014), Suppl.1, pp. 149-158
[28] Kim, D., *et al*., Modelling and Optimization of a GMA Welding Process by Genetic Algorithm and Response Surface Methodology, *International Journal of Production Research*, 40 (2002), 7, pp. 1699-1711
[29] Kumar, A., DebRoy, T., Tailoring Fillet Weld Geometry Using a Genetic Algorithm and A Neural Network Trained with Convective Heat Flow Calculations, *Welding Journal Research Supplement*, *86* (2007), 1, pp. 26-33
[30] Kumar, A., DebRoy, T., Neural Network Model of Heat and Fluid-Flow in Gas Metal Arc Fillet Welding Based on Genetic Algorithm and Conjugate Gradient Optimisation, *Science and Technology of Welding and Joining*, *11* (2006), 1, pp. 106-119
[31] Mishra, S., DebRoy, T., A Genetic Algorithm and Gradient – Descent – Based Neural Network with the Predictive Power of a Heat and Fluid-Flow Model for Welding, *Welding Journal Research Supplement, 85* (2006), 11, pp. 2315-2425
[32] Ryberg, A.-B., *et al.*, *Metamodel-Based Multidisciplinary Design Optimization for Automotive Applications*, Linkoping University Electronic Press, Linkoping, Sweden, 2012
[33] ***, No Title, https://www.mathworks.com/help/gads/paretosearch-algorithm.html
[34] Nguyen, N. T., *Thermal Analysis of Weld*s, WIT, Southampton, Boston, Mass., USA, 2004

Paper submitted: January 31, 2021
Paper revised: March 26, 2021
Paper accepted: April 2, 2021